

# Influence of the oxidation on the surface properties of silicon carbide

K. Guerfi<sup>a</sup>, S. Lagerge<sup>a,\*</sup>, M.J. Meziani<sup>a</sup>, Y. Nedellec<sup>a</sup>, G. Chauveteau<sup>b</sup>

<sup>a</sup> *Laboratoire des Agrégats Moléculaires et Matériaux Inorganiques, CNRS UMR-5072, Université Montpellier 2, Place E. Bataillon, 34095 Montpellier Cedex 5, France*

<sup>b</sup> *IFP, 1-4 avenue de Bois-Préau, BP 311, 92506 Rueil Malmaison Cedex, France*

Received 10 January 2005; received in revised form 18 January 2005; accepted 20 January 2005

Available online 25 February 2005

## Abstract

The effect of oxidation temperatures on the surface chemical properties of silicon carbide powders has been investigated. The various SiC powders have been firstly characterized using granulometry, X-ray diffraction, thermogravimetric analysis, diffuse reflectance infrared Fourier transform spectroscopy, <sup>29</sup>Si and <sup>13</sup>C MAS NMR spectroscopy. These materials seem to consist of a mixture of the 6H polytype, other polytypes β-SiC and some α-SiC. The experimental results suggest that the high-temperature treatment eliminates the graphitic region and leads to an enrichment in SiO<sub>x</sub>C<sub>y</sub> and especially SiO<sub>2</sub> units, without any important structural changes. Nitrogen and NH<sub>3</sub> gases adsorption data indicate that this conversion (from graphitic region to SiO<sub>x</sub>C<sub>y</sub> and SiO<sub>2</sub>) gives rise to an important decrease of the specific surface area while the hydrophilic character of silicon carbide powders increases. The surface density of acidic sites on SiC treated at 350, 800 and 1000 °C represents respectively about 73, 79 and 91% of the total surface sites occupied by the adsorbing NH<sub>3</sub> molecules. These information concerning the dependence of both the hydrophilic–hydrophobic character and the extent of surface acidic sites with the oxidation conditions are confirmed by immersion calorimetry experiments. Finally the calorimetric data, especially the effect of the pH on the enthalpy of immersion of SiC into water, allow additional conclusions to be drawn concerning the dependence of the electrical double layer formation with pH.

© 2005 Elsevier B.V. All rights reserved.

**Keywords:** Silicon carbide; Oxidation; Surface characterization; Immersion calorimetry; Adsorption

## 1. Introduction

Silicon carbide (SiC) exhibits a high thermostability, high mechanical strength, high heat conductivity and is a chemically inert compound up to 800 °C. Because of its chemical properties (abrasivity, semiconductor behavior, resistance to many acids), SiC is present in many applications. For instance it can be used as a catalyst support and is a promising material for a special class of electronic device applications which require extreme process conditions such as high temperatures and oxidizing environments [1]. Silicon carbide samples are also used as model for powder beds in contact with fluids [1–8] because, on the one hand, these are chemically inert against most of the usual fluids and, on the other hand, it is quite easy to get reproducible samples, especially with

respect to the chemical composition and the size distribution. As a consequence, silicon carbide is actually selected to have the main properties required for the transport of colloidal particles in model granular porous media. SiC powders are commercially available over a wide range of grain sizes. These grains have a sharp-edged shape which is characteristic of crushed mechanically isotropic materials. In all applications SiC supports (powder or wafers) are contacted with an external liquid or gaseous bulk phase. In some cases silicon carbide has to closely interact with the bulk phase or some molecular species present in it. In other cases the absence of interactions is required. It is therefore evident that a clear understanding of the surface chemistry, and surface contaminants is essential for the development of a high quality of such materials. Many studies have been undertaken to investigate (i) the surface properties, especially the effect of oxidation on the surface properties of SiC [2–8], (ii) the surface charge density using adsorption of surfactants, electrokinetic mobil-

\* Corresponding author. Tel.: +33 4 67 14 46 20; fax: +33 4 67 14 33 04.  
E-mail address: [slagerge@univ-montp2.fr](mailto:slagerge@univ-montp2.fr) (S. Lagerge).

ity measurements, titration methods, and XPS experiments [9–11], (iii) the transport of polymers under nonadsorbing [12] and adsorbing [13] conditions. The oxidation behavior is essentially controlled by the diffusion of oxidant species and it is possible to create silicon oxycarbide and SiO<sub>2</sub> species on the SiC surfaces [7,14–17]. This conversion from SiC to silicon oxycarbide and to SiO<sub>2</sub> increases with increasing the oxidation temperature and the surface area of SiC. Even if the presence of SiO<sub>2</sub> onto SiC is now evident, its surface repartition remains the topic of some debate. Indeed it is still not clear whether the SiC surface is covered by a homogeneous layer of SiO<sub>2</sub> or only exhibits SiO<sub>2</sub> sites or patches. The SiC surface is known to be heterogeneous to a greater extent than a quartzitic sand [18] and the surface charge of SiC particles in aqueous solution is slightly negative above pH 4 [19]. The adsorption of a polymer such as xanthan is negligible, whereas the adsorption of both cationic and anionic surfactants shows that 25% of the surface appears negatively charged [20]. The deposition of polystyrene latexes stabilized by grafted carboxylate functions from aqueous solutions onto passively oxidized SiC packs [21–23] suggests a significant heterogeneity in surface energy. Finally recent studies were undertaken so as to estimate the hydrophilic–hydrophobic character of various untreated and oxidized SiC surfaces [20]. The obtained data originating from (i) adsorption of molecular probes, (ii) immersion calorimetry (wetting) and (iii) flow adsorption calorimetry experiments showed important discrepancies which are discussed in details [20]. Actually the discrepancy mainly results from the fact that each experimental method involves different type of interface (solid—pure solvent (ii) and solid—solutions (i) and (iii)).

The objective of the present paper is to investigate the evolution of the physical and chemical surface properties of SiC particles with the oxidation temperature. In this attempt three different oxidation temperatures (350, 800 and 1000 °C) were applied on SiC powder and the resulting oxidized materials were characterized using several techniques: Light scattering for the determination of the particle size distributions, X-ray diffraction (XRD), thermogravimetric analysis (TGA), diffuse reflectance infrared Fourier transform spectroscopy (DRIFT), <sup>29</sup>Si and <sup>13</sup>C magic angle scanning (MAS) NMR spectroscopy and scanning electron microscopy. This first part gave information on the surface chemistry of the different samples under investigation. Then we focused on the quantification of the specific surface areas of the various SiC samples with special emphasis on the number of surface acidic sites and the hydrophilic–hydrophobic character of the surface in terms of surface energy.

## 2. Experimental

### 2.1. Solids

SiC sample (color: faded green; purity: 9%) with average particle size of 8 μm was obtained from Microlap (Ger-

many). Prior to oxidation, the powder was first washed twice with a 1 M hydrochloric acid solution for 24 h so as to remove the mineral impurities such as iron traces resulting from the grinding process. Subsequently the solid was rinsed several times with deionized water until the pH of the resulting aqueous solution remained unchanged (pH around 6.5). Finally these particles were filtrated and dried at 150 °C under vacuum (10<sup>-3</sup> Torr). The washed sample is referred to as SiC(8), where (8) indicates the average particle size in μm. Afterwards, the SiC(8) particles were oxidized for 8 h at 350, 800 and 1000 °C under ambient atmosphere so as to obtain three oxidized powdered materials referred to as SiC(8)350, SiC(8)800 SiC(8)1000, respectively. An additional sample, referred to as SiC(8)800pH13, was also obtained by oxidation of SiC powder at 800 °C (SiC(8)800) with subsequent chemical treatment with a NaOH solution at pH 13. The NaOH treatment of SiC(8)800 was carried out in a polypropylene beaker by mixing 5 g of SiC(8)800 in 250 ml of NaOH solution at pH 13 for 24 h. Subsequently, the resulting SiC sample was rinsed several times with deionized water until the pH of the resulting aqueous solution remained unchanged (pH around 6.5) and then filtrated and dried at 150 °C under vacuum (10<sup>-3</sup> Torr).

Samples of amorphous silica Aerosil 300 from Degussa AG and graphite powder (1–2 μm) from Aldrich have been investigated together with the SiC samples for comparison.

Particle size distributions of silicon carbide particles in dilute suspension (10<sup>-4</sup>, v/v) in deionized water at pH 6.5 were measured by light scattering using a Mastersizer apparatus (Malvern Instrument). The analysis showed relatively narrow particle size distributions with average diameters ( $d_a$ ) reported in Table 1. The oxidation at 350, 800 and 1000 °C and NaOH treatments did not significantly affect the average diameter of the particles.

For each solid sample, the BET specific surface area ( $S_{BET}$ ) was determined from N<sub>2</sub> gas adsorption measurements at 77 K using an automated volumetric apparatus (Micromeritics ASAP 2010) taking the surface area per nitrogen molecule as 0.162 nm<sup>2</sup> and by application of the BET equation [32,33]. Prior to the adsorption measurements, all samples were heat treated at 423 K under vacuum (10<sup>-5</sup> Torr) for 5 h. Evolution of the BET specific surface area ( $S_{BET}$ ) of

Table 1  
Average diameter ( $d_a$ ), BET surface area ( $S_{BET}$ ), BET constant ( $C_{BET}$ ) and total ( $\Gamma_{tot}$ ) and irreversible ( $\Gamma_{irr}$ ) adsorption obtained for silicon carbide powders after oxidation at different temperatures and after NaOH treatment

	Solid			
	SiC(8)350	SiC(8)800	SiC(8)1000	SiC(8)800pH13
$d_a$ (μm)	9.0	10.5	11.5	11.2
$S_{BET}$ (m <sup>2</sup> g <sup>-1</sup> )	1	0.6	0.6	0.6
$C_{BET}$	154	235	1000	78
$\Gamma_{tot}$ (μmol m <sup>-2</sup> )	7.4	14	22.0	
$\Gamma_{irr}$ (μmol m <sup>-2</sup> )	5.4	11	20.0	

$S_{BET}$  and  $C_{BET}$  were obtained from Nitrogen adsorption experiments whereas ( $\Gamma_{tot}$ ) and ( $\Gamma_{irr}$ ) refer to ammonia adsorption.

the SiC samples as a function of the oxidation treatment and the related BET energetic constant ( $C_{\text{BET}}$ ) are presented in Table 1.

## 2.2. Surface characterization

X-ray powder diffraction (XRD) data were acquired on an automated Philips diffractometer using Cu K $\alpha$  radiation. Thermogravimetric analysis was performed in dry air using a Stanton STA 781 thermal analyzer operating at a heating rate of 2° min<sup>-1</sup>. Diffuse reflectance infrared Fourier transform spectroscopy (DRIFT) has been carried out on a Nicolet Magna 550 using a data spacing of 1 cm<sup>-1</sup>. A mixture of SiC in KBr (dilution about 100 times) has been used to identify the surface groups of the SiC powders. NMR spectra were obtained with a Bruker spectrometer operating at a frequency of 59.627 MHz for <sup>29</sup>Si and 75.468 MHz for <sup>13</sup>C. <sup>29</sup>Si spectra were measured without cross-polarization to protons and with MAS.

The number of surface acid sites was evaluated by two adsorption cycles of ammonia from gas phase [36]. The amount of NH<sub>3</sub> adsorbed ( $\Gamma$ ) as a function of the partial pressure ( $P$ ) in the equilibrium bulk phase was measured using Micromeritics ASAP 2010 Chemi System apparatus which allowed the adsorption isotherms ( $\Gamma = f(P)$ ) to be constructed. Prior to the adsorption measurements, the SiC samples (about 5 g) were outgassed at 433 K under vacuum (10<sup>-5</sup> Torr) for 5 h so as to standardize the surface state and eliminate all the physisorbed water. Then successive ammonia aliquots were contacted with the sample until a final equilibrium pressure around 40 Torr in the bulk phase was reached. The equilibrium pressure ( $P$ ) was measured after each adsorption step and the corresponding amount of NH<sub>3</sub> adsorbed ( $\Gamma$ ) was calculated. At the end of the first adsorption cycle ( $P = 40$  Torr), the sample was outgassed under vacuum at 373 K for 30 min (desorption cycle) and a second adsorption cycle was then performed in the same conditions.

Immersional wetting calorimetric measurements were used so as to quantify the strength of the interactions between the SiC surface and different pure liquids [37]. This method especially allowed us to determine the enthalpies of immersion ( $\Delta_{\text{imm}}H$ ) of the adsorbent into different solvents, i.e. the enthalpy change resulting from the creation of the solid-liquid interface. The investigated immersion liquids were water, one partly polar solvent (formamide) and one non-polar solvent (*n*-heptane). The used conduction calorimeter and its operational procedure have been widely described previously [38,39]. The solid sample was initially heated at 433 K under vacuum (10<sup>-3</sup> Torr) for five hours so as to standardize the surface state.

## 3. Results and discussion

The results of X-ray diffraction patterns of SiC(8)350, Aerosil 300 and graphite are displayed in Fig. 1. The X-ray

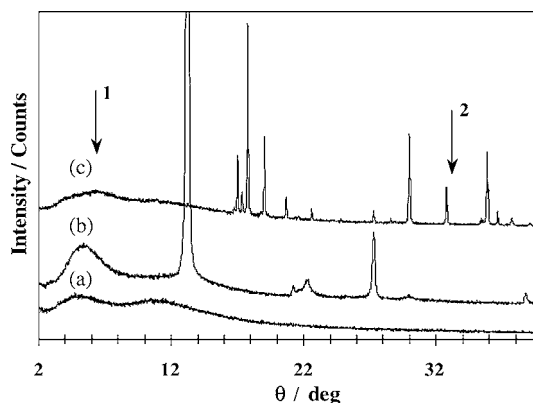


Fig. 1. X-ray diffraction patterns of Aerosil 300 (a), graphite (b) and SiC(8)350 (c).

diffractograms of amorphous silica Aerosil 300 and graphitic powder samples are included for comparison. Whatever the treatment of SiC, XRD diffraction lines remained unchanged. All SiC samples exhibit diffraction lines which correspond to  $\beta$ -SiC crystallized in the moissanite-6H type [24]. In addition to the  $\beta$ -SiC diffraction lines, a slight broad peak located at low theta angle (arrow 1) is also observed for all samples, which could be attributed to both the unreacted remaining carbon and SiO<sub>2</sub> structures with a short-range periodicity. It is also possible that small amounts of  $\alpha$ -SiC are present along with  $\beta$ -SiC, which is evidenced by a peak located at diffraction angles around 34° (arrow 2). This diffraction line is ascribed to  $\alpha$ -SiC in the 4H and 15R structures. The SiO<sub>2</sub> species, if present, are probably only in an amorphous form or in very small amounts.

The thermogravimetric analysis (TGA) of all SiC samples recorded under air are presented in Fig. 2. Two distinct stages of weight gain in the TGA data are observed, i.e. in the range between 25 and 750 °C and above between 750 and 1000 °C. The first weight gain changes from 0.2% for SiC(8) to about 0.3–0.4% for the other materials. The second one above 750 °C all the more increases as the oxidation temperature raises. At 1000 °C, the weight gain is close to 1.6% for

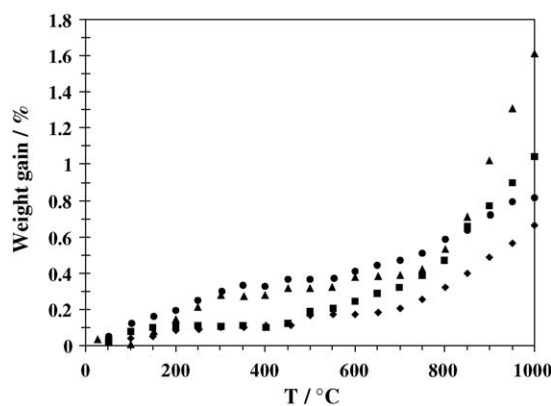
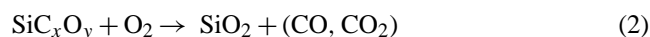


Fig. 2. Thermogravimetry analysis of SiC(8) (◆), SiC(8)350 (■), SiC(8)800 (▲) and SiC(8)800pH13 (●).

SiC(8)800, while it is about 0.6% for SiC(8). After NaOH treatment the 1000 °C weight gain of the SiC(8)800 sample falls down around 0.8% (SiC(8)800pH13) which is close to the value observed for SiC(8)350. In the 25–750 °C temperature range, one can assume that CO<sub>2</sub> and H<sub>2</sub>O are eliminated following oxidation while a slight intake of oxygen is occurring. However, the departure of both gases originating from the combustion of free carbon following the below reaction (1) should give rise to a weight loss and thereby is not consistent with the weight gain observed in the TGA experiments. Consequently, the observed weight gain seems more related with the prevailing oxidation process of both the silicon oxycarbide and silicon carbide phases according to the reactions (2) and (3)



Above 750 °C, the weight gain observed for SiC(8)800 drastically increases compared to the others samples, which suggests that the oxidation of silicon oxycarbide (favored at high temperature) having different surface compositions is easier than that of silicon carbide. As discussed by Bermudez [25], at elevated temperature, the adsorbed oxygen atoms undergo structural rearrangement and migrate to more stable sites; these probably displace carbon atoms from SiC and preferentially accommodate themselves in those vacant sites to form SiO<sub>2</sub> [26]. After NaOH treatment (SiC(8)800pH13), the slight value of final weight gain can be ascribed to the dissolution of the SiO<sub>2</sub> or SiC<sub>x</sub>O<sub>y</sub> layer initially formed onto SiC(8)800. The immersion calorimetry data obtained for the same solid surfaces, which will be described in the following section, may lead to a clue to supporting such an oxidation process. Generally, the oxidation behavior seems to be different, certainly because of different microstructure. Whatever the treatment temperature is, 350 or 800 °C, these materials reveal a good resistance to oxidation.

Fig. 3 shows the results of DRIFT analysis obtained for various SiC samples and Aerosil 300. Results for amorphous silica Aerosil 300 are reported for comparison (curve e). The DRIFT spectra of all SiC samples are very similar and exhibit almost the same absorption bands. Both absorption bands at 790 and 900 cm<sup>-1</sup> originate from Si–C vibration, whereas the band around 1100 cm<sup>-1</sup> is due to the asymmetric stretching vibration of Si–O bonds as confirmed by the spectrum of amorphous silica (curve e) [27]. The bands at 1270 and 1360 cm<sup>-1</sup> can be attributed to the vibrations of the CH<sub>2</sub> groups in Si–CH<sub>2</sub>–CH<sub>3</sub> and Si–CH<sub>2</sub>–Si groups [28]. Finally the band ascribed to water is around 1630 cm<sup>-1</sup>. This band with that around 1550 cm<sup>-1</sup> could also reflect the asymmetric vibration of C–C bonds into the graphite carbon. After oxidation of SiC(8) at 800 °C, an absorption of minor intensity arises at 1100 cm<sup>-1</sup> indicating the presence of some SiO<sub>2</sub> species according to curve e. This absorption

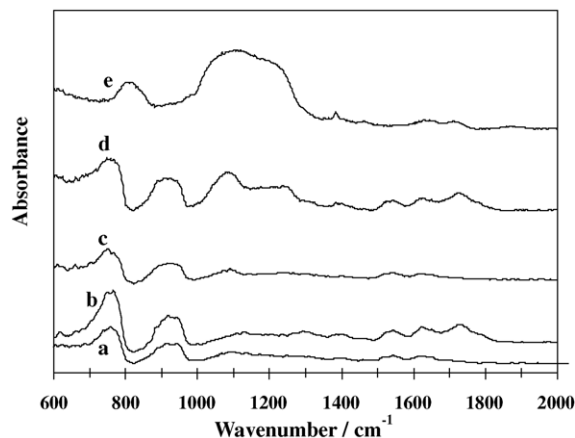


Fig. 3. DRIFT spectra of SiC(8)800pH13 (a), SiC(8)350 (b), SiC(8)800 (c), SiC(8)1000 (d) and Aerosil 300 (e).

is more pronounced after oxidation at 1000 °C. This later band at 1100 cm<sup>-1</sup> is very small for SiC(8)350 (curve b) suggesting a very small extent of SiO<sub>2</sub> layer on the sample. It is evident that the NaOH treatment (SiC(8)800pH13) causes the dissolution of the SiO<sub>2</sub> layer as indicated by the absence of Si–O absorbance on curve a. The spectrum obtained with SiC(8)800pH13 rather resembles to that obtained with SiC(8)350. Finally the DRIFT analysis obtained for SiC(8) was quite identical to that obtained with SiC(8)350 and thereby is not presented in Fig. 3.

NMR spectroscopy can bring further information about the local environment for silicon and carbon atoms. The <sup>29</sup>Si MAS NMR spectra of SiC(8)350, SiC(8)800, SiC(8)800pH13 and SiC(8)1000 are shown in Fig. 4. These spectra exhibit three main resonances at –14, –20 and –25 ppm with different intensity. As reported previously for a 6H material [29–31], the silicon NMR spectrum also presents three resonances which have quite the same intensity, at –16, –22 and –27 ppm. Following oxidation at 800 °C, the silicon MAS spectrum of the oxidized sample (Fig. 4, curve b) is essentially the same as that observed before the oxidation,

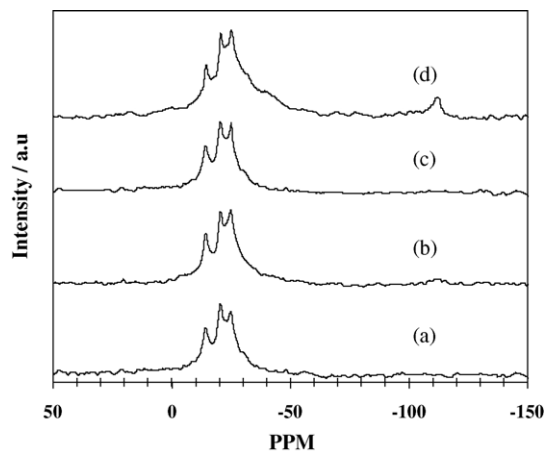


Fig. 4. <sup>29</sup>Si MAS NMR spectra of SiC(8)350 (a), SiC(8)800 (b), SiC(8)800pH13(c), and SiC(8)1000 (d).



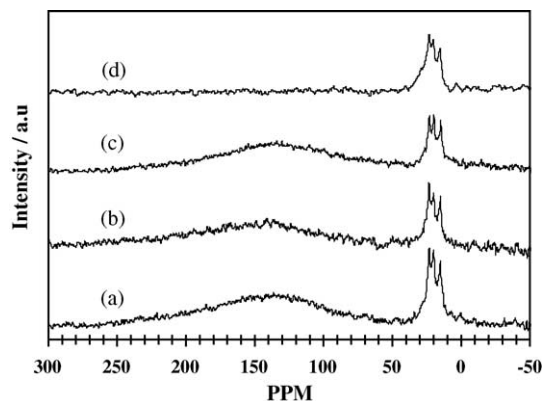


Fig. 5.  $^{13}\text{C}$  MAS NMR spectra of SiC(8)350 (a), SiC(8)800 (b), SiC(8)800pH13(c), and SiC(8)1000 (d).

but with a shoulder on the low-field peak around  $-40$  ppm and a very weak resonance around  $-115$  ppm compared to the SiC(8). SiC(8)800 treated with NaOH (SiC(8)800pH13 (curve c)) displays almost similar  $^{29}\text{Si}$  spectrum (curve c) as non-treated. The main difference is the absence of weak resonance around  $-115$  ppm attributed to the silicon oxide present on the SiC. This result confirms the dissolution of silicon oxide after NaOH treatment.

The literature also reports that the carbon MAS exhibits three resonances at  $+23$ ,  $+20$  and  $+15$  ppm, attributed to carbidic carbons in this structure [29–31]. The  $^{13}\text{C}$  MAS presented in Fig. 5 shows three peaks at  $+24$ ,  $+20$  and  $+16$  ppm and a broad resonance around  $140$  ppm, except for SiC(8)1000, probably due to the presence of graphite in the carbon core. The later peaks can be assigned to the Si-CH<sub>2</sub>-CH<sub>3</sub> and Si-CH<sub>2</sub>-Si groups on the surface. Hence, the various resonance positions strongly suggest that the investigated materials consist of a mixture of the 6H polytype, other polytypes  $\beta$ -SiC (as shown from the above RX analysis) and a very small fraction of  $\alpha$ -SiC, detectable from the underlying feature. The carbon MAS spectrum maintains the same peaks for all the samples but the intensity of a broad resonance around  $140$  ppm is reduced, as compared with the sample before treatment. The  $^{13}\text{C}$  spectrum of SiC(8)800 treated with NaOH (curve c) is very similar as that obtained with the non-treated sample. After oxidation at  $1000^\circ\text{C}$ , several changes in the  $^{29}\text{Si}$  and  $^{13}\text{C}$  spectra are apparent (curves 4d and 5d). In Fig. 4 (curve d), resonances near  $-40$ ,  $-75$  and  $-115$  ppm can indicate the presence in the sample of SiC<sub>2</sub>O<sub>2</sub>, SiCO<sub>3</sub> and high amount of silicon oxides, respectively. Fig. 5 (curve d) does not display broad resonance around  $140$  ppm assigned to the graphitic carbons. The treatment at high temperature extensively removes the graphitic region from the SiC phase and creates some silicon oxycarbide sites and an important amount of silicon oxide.

Evolution of the BET specific surface area ( $S_{\text{BET}}$ ) of the SiC samples as a function of the oxidation treatment and the related BET energetic constant ( $C_{\text{BET}}$ ) are presented in Table 1. According to the isotherm classification [32,33], all

the shapes of adsorption–desorption isotherms were found to be of type II indicating the absence of the porous structure. With increasing the temperature reaction, the materials surface areas decrease. The  $S_{\text{BET}}$  strongly decreases after oxidation at  $800^\circ\text{C}$ , but remains constant between  $800$  and  $1000^\circ\text{C}$ . The constant  $C_{\text{BET}}$  which is related to the heat of adsorption also increases significantly, especially between  $800$  and  $1000^\circ\text{C}$ . These  $C_{\text{BET}}$  values are mainly related to the energetic activity of the surface, and are particularly influenced by the polar character of the surface. The interaction between the adsorbed nitrogen molecules and the surface sites increases with the hydrophilic character (temperature treatment) of the surface and the resulting adsorption heat is enhanced. On this basis, the results in Table 1 clearly indicate that the oxidation at elevated temperature enhances the surface hydrophilicity of silicon carbide. Such a phenomenon was already reported in the literature [34,35] and was ascribed to the surface diffusion process. The authors have shown that SiC started to sinter by surface diffusion at temperature lower than the theoretical sintering temperature. The decrease in surface area after oxidation could be due either to the formation of an amorphous silica layer on the SiC surface or to the effect of agglomeration between very fine particles. The first hypothesis is rejected because the BET surface area of SiC(8)800 ( $0.6\text{ m}^2\text{ g}^{-1}$ ) remains unchanged after NaOH treatment (SiC(8)800pH13). Indeed this NaOH treatment allows most of the silica or oxycarbide layers present on the SiC surface to be removed. Consequently, the only factor responsible for the reduction of the BET surface area is the agglomeration between the very fine particles after oxidation.

The adsorption measurements of gaseous NH<sub>3</sub> onto different samples of SiC have been quantified so as to evaluate the number of surface acidic sites. Ammonia is a reliable basic probe molecule for surface acidity testing on account of its small cross-sectional area ( $0.14\text{ nm}^2$ ) and suitable  $pK_{\text{a}} = 9.24$  [36]. Fig. 6 shows the NH<sub>3</sub> adsorption isotherms obtained in two successive adsorption cycles for SiC(8)350, SiC(8)800 and SiC(8)1000. The difference between both adsorption values has also been plotted versus the equilibrium bulk pressure.

The first cycle isotherms of NH<sub>3</sub> adsorption show important difference between the different SiC samples concerning the amounts of adsorption. As a general trend, the total amount adsorbed increases very quickly with increasing the bulk pressure in the region of very low pressures ( $<5$  Torr). This indicates the presence of numerous acidic surface sites, which give strong acid–base interactions with ammonia molecules. For relatively higher pressure values ( $>5$  Torr), the rate of increasing adsorption on both samples decreases and the adsorption isotherms become quasi linear. This linear tendency may be explained by the physical adsorption and even the formation of multilayer, following or paralleling to the NH<sub>3</sub> chemisorption on acidic sites. The slopes of the linear segments are similar for all three systems which indicates that physical adsorption of ammonia molecules progresses in the same way. Both straight lines obtained from both adsorption isotherms (one corresponding

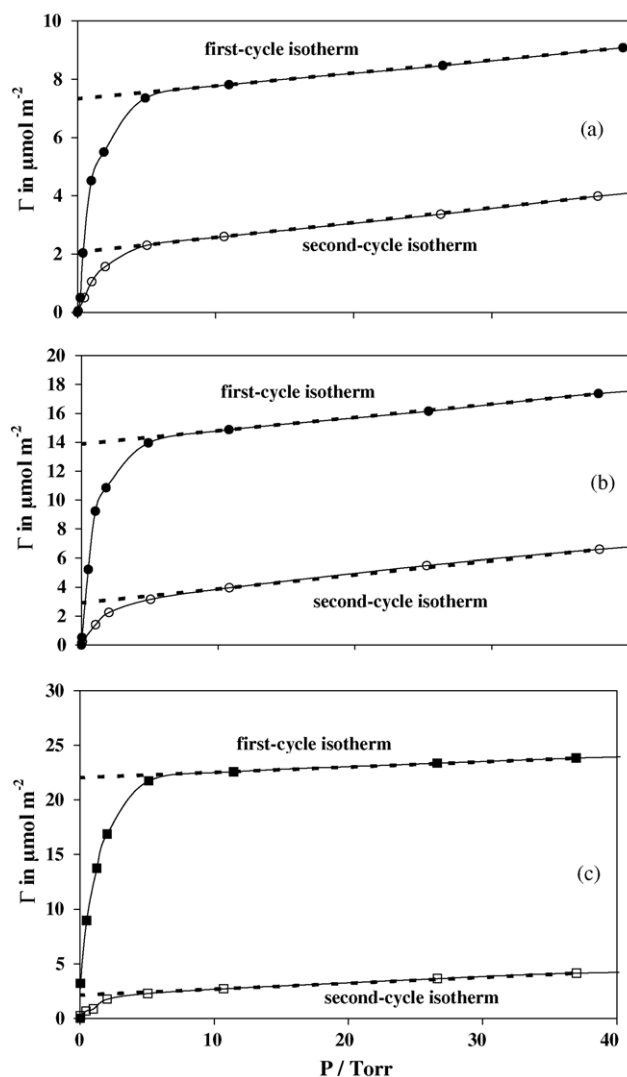


Fig. 6.  $\text{NH}_3$  adsorption isotherms obtained in two successive adsorption cycles: SiC(8)350 (a), SiC(8)800 (b) and SiC(8)1000 (c).

to the first adsorption cycle and the other obtained after the outgassing (second adsorption cycle)) are suitably extrapolated to zero pressure. The difference between these two extrapolated values determines the maximum amount of  $\text{NH}_3$  molecules which is irreversibly adsorbed,  $\Gamma_{\text{irr}}$ , on the silicon carbide surface.  $\Gamma_{\text{irr}}$  reflects the localized chemisorption of single ammonia molecules on acidic surface sites and consequently provides the total number of such sites on the solid surfaces. The amount of the adsorbate irreversibly retained on the SiC surfaces ( $\Gamma_{\text{irr}}$ ) are given in Table 1. These reported values allowed the surface density of acidic surface sites on SiC(8)350, SiC(8)800 and SiC(8)1000 samples to be assessed. These were found to correspond to 73, 79 and 91% ( $\Gamma_{\text{tot}}/\Gamma_{\text{irr}}$ ), respectively, of the total surface sites occupied by the adsorbing  $\text{NH}_3$  molecules ( $0.14 \text{ nm}^2$ ). It is clear that the number of surface acidic sites is markedly increased when the silicon carbide is oxidized at 800 and 1000 °C. This oxidation can provide many Lewis acid and Brönsted acid surface

Table 2

Enthalpies of immersionsal wetting of the silicon carbide samples in *n*-heptane, water and formamide

Solid	$S_{\text{BET}}$ ( $\text{m}^2 \text{ g}^{-1}$ )	$\Delta_{\text{imm}}H$ ( $\text{mJ m}^{-2}$ )		
		Heptane	Water	Formamide
SiC(8)	1	425	428	473
SiC(8)350	1	637	465	551
SiC(8)800	0.6	1047	710	895
SiC(8)1000	0.6	957	969	1177
SiC(8)800pH13	0.6	1111	565	940
SiC(8)800HF	0.8	868	440	720
Aerosil300	280	97	160	217
Graphite	13.2	331	225	350

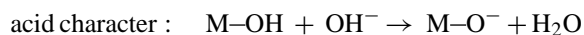
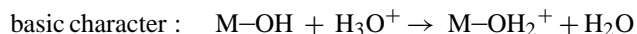
Particles with average diameters of 2 and 8  $\mu\text{m}$  were used. Results obtained with graphite and silica Aerosil 300 are given for comparison. Finally SiC(8)800HF was obtained from SiC(8)800 after treatment in fluorydric acid.

sites originating from Si–O–C and Si–O–Si bridging oxygen atoms, and different hydroxyl species.

The influence of the oxidation conditions on the enthalpy of immersionsal wetting of the silicon carbide samples are reported in Table 2. These results clearly show that the SiC surfaces exhibit an hydrophilic–hydrophobic partition. The high enthalpic values obtained following immersion of the solid in water and formamide indicate that a significant fraction of the BET solid surface presents a significant hydrophilic character. In each case, the enthalpies of immersionsal wetting in formamide are higher than those obtained in water. This is mainly due to the strong basic character of the formamide molecule compared to water, and consequently reflects the occurrence of acid sites on the solid surfaces. High enthalpic values are also observed following immersion into *n*-heptane. These mainly originate from van der Waals interactions and thereby also indicate the presence of a significant hydrophobic character of the oxidized silicon carbide surfaces. Table 2 clearly evidences that the oxidation of SiC samples leads to an increase of the enthalpy of immersionsal wetting in a similar way with the three different immersionsal solvents. After NaOH treatment at pH 13 (SiC(8)800pH13), the enthalpy of immersionsal wetting determined in water decreases (–25%) while those obtained in formamide and *n*-heptane remain quite unchanged (895/940 and 1047/1111, respectively). The observed differences before and after NaOH treatment are around 5–6% which is the order of magnitude of the experimental error. As a consequence, it is probable that the acidic surface sites are mainly  $\text{SiC}_x\text{O}_y$  groups and that these sites are not removed following NaOH treatment. Finally, after HF (SiC(8)800HF) treatment, a significant decrease of the enthalpic values is observed in every cases (water, formamide and *n*-heptane). This decrease is much more marked in the case of water (–38%) than in the case of *n*-heptane and formamide (around –17–20%). These declining enthalpic values, especially related with water, are probably due to the dissolution of active groups such as  $\text{SiO}_2$  from the solid surface following the NaOH and HF treatments. Moreover NaOH treatment is quite soft compared with HF

treatment. Consequently, it is probable that, following NaOH treatment, only surface active groups such as  $\text{SiO}_2$  are concerned, while, following HF treatment, the surface state of the SiC sample is significantly modified as supported by the increase of the BET surface area from  $0.6$  to  $0.8 \text{ m}^2 \text{ g}^{-1}$ . In the latter case the strong acidic attack significantly modifies the physical, chemical and textural properties of the SiC surface accounting for the enthalpic decrease also observed in the case of formamide and *n*-heptane. Finally if we compare the immersion enthalpies for SiC with other obtained with the graphite and the silica Aerosil 300, it is surprising to note that the SiC surfaces give very high enthalpic values. Such a magnitude was never observed previously with several hydrophilic and hydrophobic divided solids.

Most of the solid surfaces may develop a heterogeneous electrical interface following their immersion in water. In the case of mineral oxides, the surface charge is generally made of ionized hydroxyl groups which behave and may react as weak acid and bases as a function of the pH solution according the following equilibria:



The resulting surface charge will depend on the pH value, and is globally zero at a particular value of the pH that is called point of zero charge (PZC). Previous work performed by Fuerstenau and coworker [40,41] on the effect of the pH on the enthalpy of immersion of alumina into water, showed the occurrence of an enthalpic contribution corresponding to the formation of the electrical double layer which depends on the pH value. This effect was ascribed to the formation of the negatively and positively charged surface sites,  $\text{Al-O}^-$  or  $\text{Al-OH}_2^+$ , and to the formation of a monolayer of water strongly interacting with the alumina surface through hydrogen bonds. However, at high pH values, the measured enthalpic effect may reflect several other phenomena, especially the eventual dissolution of the divided solids and the presence of counter-ions that greatly disturb the electrical double layer. In this study we have investigated the dependence of the enthalpy of immersionsal wetting with the pH value of the immersionsal aqueous phase so as to better elucidate this problem. The immersion experiments were applied to different SiC samples oxidized at different temperatures. SiC is particularly stable and resistant at high pH values and do not dissolve under these high-pH conditions. Oxidation of SiC samples at high temperature allows a surface oxide film to be formed.

Fig. 7 shows the evolution of the immersion enthalpy of SiC(8), SiC(8)350, SiC(8)800 and SiC(8)1000 as a function of the pH of the aqueous immersionsal solution. All three curves exhibit a very similar trend (parabolic shape) with the occurrence of three different regions independently of the oxidation conditions. In the range of low pH values ( $\text{pH} < 2.5$ ), the enthalpic values slightly decline as the pH increases. For relatively higher pH values ranging between 2.5 and 11,

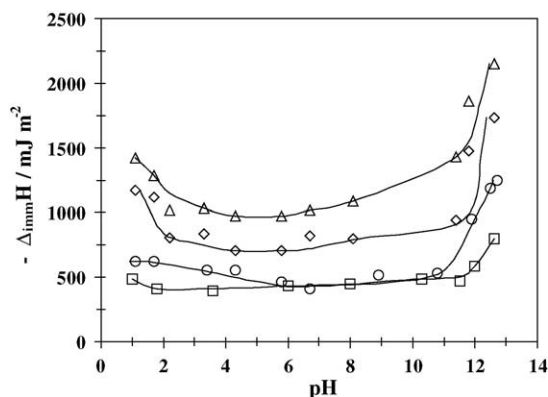


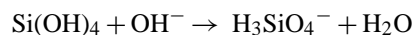
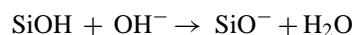
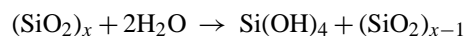
Fig. 7. Variation of the enthalpy of immersionsal wetting as a function of the pH. SiC(8) ( $\square$ ), SiC(8)350 ( $\circ$ ), SiC(8)800 ( $\diamond$ ), SiC(8)1000 ( $\triangle$ ).

the enthalpies of immersionsal wetting stabilize to minimal values which are quite close to the enthalpy of immersion into water ( $\text{pH} \approx 6$ ). Finally for  $\text{pH} > 11$ , the enthalpic curves drastically increase up to final values (at  $\text{pH} = 13$ ) which are more than twice higher than that obtained in water ( $\text{pH} \approx 6$ ). It is interesting to note that the main differences between SiC(8) (non-oxidized) and SiC(8)350 (oxidized at  $350^\circ\text{C}$ ) are only observed at high pH values ( $\text{pH} > 11$ ). Increasing the oxidation temperature from  $350^\circ\text{C}$  (SiC(8)350) to  $1000^\circ\text{C}$  (SiC(8)1000) gives rise to an increase of the immersion enthalpy in the whole range of pH values.

The immersion enthalpy in the pH range between 2.5 and 11 may be ascribed to the following two contributions: (i) formation of a few charged surface sites and (ii) physisorption of water molecules both onto these newly formed active sites and onto the surface. It has been shown that, in this pH range, the SiC surface charge does not change significantly following pH variations indicating that the effect of the double layer formation on the enthalpic value is not the prevailing contribution. As a consequence, the increase of the immersion enthalpy with oxidation of the SiC surface may result from the strong interaction between physisorbed water and the freshly formed active sites of the oxidized surface. In such a case, the increase of the oxidation temperature (from 350 to  $1000^\circ\text{C}$ ) favors the formation of surface active groups and thereby the water molecules tend to form a more and more strongly interacting water monolayer on the oxidized surface. The presence of hydrogen bonds between the surface active sites created following oxidation ( $\text{SiC}_x\text{O}_y$  and  $\text{SiO}_2$ ) and the water molecules coordinated in a tetrahedral way may be responsible for the high stability of the adsorbed layer. This strong binding may further lead to the formation of additional water layers.

In the extreme range of pH values ( $\text{pH} < 2.5$  and  $\text{pH} > 11$ ), the enthalpy of immersionsal wetting reflects the ionization of the surface hydroxyl groups i.e., the double layer formation. In addition to the two above described contributions, the immersion enthalpy in these pH ranges may be considered as resulting from four superimposed effects whose extent depends on the pH value. (1) Formation of a charged surface

with a given charge density at a given pH, (2) interaction between charged surface active sites as these become more numerous, (3) counter-ions interactions in the double layer, and (4) dissociation of the surface. No differences were observed on the measured enthalpy following immersion of SiC powders in solutions containing different amount of electrolyte (extra salt NaCl). This suggests a very weak effect for the counter-ions interaction in the double layer. The most important and prevailing effects are (1) and (4). At  $\text{pH} > 11$ , the silica layer that is formed following oxidation not only develops a negative surface charge (ionization of OH groups) but also partially dissolves with formation of silicates ions according the following equilibria:



In Fig. 8, we have reported similar results obtained with silica Aerosil 300, silica XOB015 and a graphite powder. Fig. 8 also shows the solubility behavior of an amorphous silica (black circles) as a function of the equilibrium pH. Concerning the enthalpic curves, a similar parabolic trend is observed with much lower enthalpies. The immersion enthalpy of graphite powder only increases at  $\text{pH} < 4$ . In the range of  $\text{pH} > 4$ , this enthalpy stabilizes around  $225 \text{ mJ m}^{-2}$  and slightly increases at  $\text{pH} > 12$ . The immersion enthalpy of silica XOB015 is higher than that of silica Aerosil 300 in the whole range of pH values due to the presence of more active and energetic hydroxyl surface sites onto the hydrophilic silica XOB015. Such active surface sites favor the formation of a strongly bound monolayer of water on the surface through hydrogen bonds. Basing on the pH-solubility dependence (black circles), it is probable that the increasing immersion enthalpy

generally observed, especially at  $\text{pH} > 10.5$ , may be ascribed to the dissolution of the silica. However, the steeply rising parts of the enthalpic curves start for pH slightly higher compared to the dissolution curve. This phenomenon is probably due to the absence of stirring during the immersion process. The difference in the immersion enthalpy between  $\text{pH} = 10$  and 12.5 does not exceed 200 and  $250 \text{ mJ m}^{-2}$  for the amorphous silica and the silica XOB015, respectively. Comparison of these values with those obtained for SiC(8)800 (around  $800 \text{ mJ m}^{-2}$ ) suggests that the formed silica layer is identical neither to an amorphous silica nor to a silica XOB015. It is thus possible that this silica layer is composed by a mixture of active sites such as  $\text{SiC}_x\text{O}_y$  and  $\text{SiO}_2$  making the surface more energetic at high pH values. The charged surface sites originating from such  $\text{SiC}_x\text{O}_y$  groups and their dissolution are more energetic at high pH. Finally this behavior may be explained basing on the concept of both the chemical and physical hardness of the solid supports. The chemical hardness is defined as the ability of the material to resist to the change in the electronic distribution, while the physical hardness provides a measure of the resistance of the material to change in the nuclear position. Both properties affect the adhesion behavior of the materials. The elevated enthalpy of immersion of SiC compared to the other divided solids is associated with the elevated hardness of the SiC sample which make this adhesion more energetic.

#### 4. Conclusion

The silicon carbide samples treated under different oxidation temperatures (350, 800 and  $1000^\circ\text{C}$ ) show the same structure composed by the mixture of 6H polytype, polytypes  $\beta$ -SiC and some  $\alpha$ -SiC in the 4H and 15R structures, as observed by X-ray diffraction.  $\text{SiO}_2$  species is also present and probably in an amorphous form. One of the most important characteristic of such solid supports is the high thermal stability in non-oxidizing environments. Oxidation in air at elevated temperatures has been analyzed by different techniques (thermogravimetric and DRIFT analysis,  $^{29}\text{Si}$  MAS NMR and  $^{13}\text{C}$  MAS spectroscopy) and is shown to cause substantial SiC conversion into  $\text{SiO}_x\text{C}_y$  and  $\text{SiO}_2$ . For all SiC samples a prevailing oxidation process of both the silicon oxycarbide and silicon carbide phases occurs at quite low temperature (between 25 and  $750^\circ\text{C}$ ). After oxidation at  $800^\circ\text{C}$  the presence of some  $\text{SiO}_2$  species is detected on the solid surface. The treatment at high temperature extensively removes the graphitic region from the SiC phase and creates some silicon oxycarbide sites and an important amount of silicon oxide. After oxidation at  $1000^\circ\text{C}$  the presence in the sample of  $\text{SiC}_2\text{O}_2$ ,  $\text{SiCO}_3$  and high amount of silicon oxides ( $\text{SiO}_2$ ) was evidenced. However a very small extent of the  $\text{SiO}_2$  layer was found on the sample oxidized at  $350^\circ\text{C}$ . This  $\text{SiO}_2$  layer is dissolved following NaOH treatment. The oxidation of silicon oxycarbide having different compositions is more easier than that of silicon carbide. This conversion

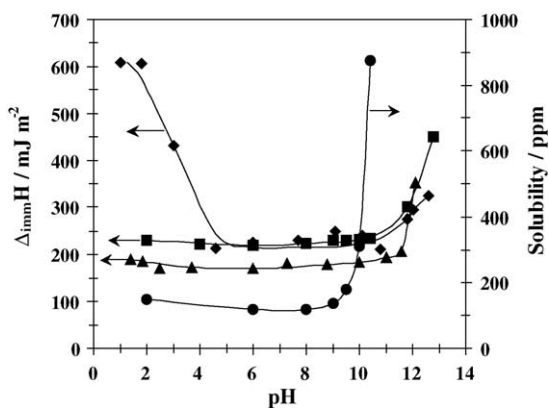


Fig. 8. Variation of the enthalpy of immersionsal wetting of different solid samples as a function of pH: precipitated crystalline silica XOB015 (■), pyrogenic silica Aerosil (▲), and graphite powder (◆) and evolution of the solubility of Amorphous silica (●) against the pH.



leads to an important decrease of specific surface area particularly between sample oxidized at 350 and 800 °C probably attributed to the effect of agglomeration between very fine particles after oxidation. All the transformation from silicon carbide to  $\text{SiO}_x\text{C}_y$  and  $\text{SiO}_2$  cause a significant enhancement of the hydrophilic character of silicon carbide powders. This feature is also evidenced from  $\text{N}_2$  adsorption data. Indeed, the interaction between the adsorbed nitrogen molecules and the surface sites increases with the hydrophilic character of the surface. This interaction is reflected by the constant  $C_{\text{BET}}$  which increases significantly with the oxidation temperature of SiC samples. This clearly indicates that the oxidation at elevated temperature enhances the surface hydrophilicity of silicon carbide, especially between 800 and 1000 °C.

Adsorption measurements of gaseous  $\text{NH}_3$  onto the investigated samples of SiC indicate the presence of numerous acidic surface sites. Irreversible adsorption of  $\text{NH}_3$  reflects the localized chemisorption of single ammonia molecules on acidic surface sites and consequently provides the total number of such sites on the solid surfaces. The surface density of acidic sites on SiC powders oxidized at 350, 800 and 1000 °C were found to represent about 73, 79 and 91%, respectively, of the total surface sites occupied by the adsorbing  $\text{NH}_3$  molecules. It is clear that the number of surface acidic sites is markedly increased when the silicon carbide is oxidized at 800 and 1000 °C. This oxidation can provide many Lewis acid and Brønsted acid surface sites originating from Si–O–C and Si–O–Si bridging oxygen atoms, and different hydroxyl species.

The hydrophilic character dependence with the oxidation conditions is supported by calorimetric results of immersion of the SiC samples in water and formamide. Moreover the enthalpies of immersion obtained in formamide also support the occurrence of acid sites on the solid surfaces. It is probable that the acidic surface sites are mainly  $\text{SiC}_x\text{O}_y$  groups and that these sites are not removed following NaOH treatment. Only  $\text{SiO}_2$  are concerned with the NaOH treatment.

Finally, the evolution of the immersion enthalpy of SiC oxidized under different conditions as a function of the pH of the aqueous immersional solution allows some additional information to be drawn. The increase of the oxidation temperature (from 350 to 1000 °C) favors the formation of surface active groups and thereby the water molecules tend to form a more and more strongly interacting water monolayer on the oxidized surface. The presence of hydrogen bonds between the surface active sites created following oxidation ( $\text{SiC}_x\text{O}_y$  and  $\text{SiO}_2$ ) and the water molecules coordinated in a tetrahedral way may be responsible for the high stability of the adsorbed layer. In the extreme range of pH values ( $\text{pH} < 2.5$  and  $\text{pH} > 11$ ), the enthalpy of immersion reflects the ionization of the surface hydroxyl groups i.e., the double layer formation. The most important and prevailing contribution to the observed immersion enthalpy in these pH ranges is supposed to be the formation of a charged surface with a given charge density at a given pH (dissociation of the surface groups). Calorimetric data obtained with two silica samples

were compared with those obtained for with oxidized SiC samples and suggest that the formed silica layer is identical neither to an amorphous silica nor to a crystalline silica. It is thus possible that this silica layer is composed by a mixture of active sites such as  $\text{SiC}_x\text{O}_y$  and  $\text{SiO}_2$  making the surface more energetic at high pH values.

## References

- [1] M.A. Vannice, Y.-L. Chao, R.M. Friedman, *Appl. Catal.* 20 (1986) 91–107.
- [2] G. Ervin Jr., *J. Am. Ceram. Soc.* 41 (1958) 347–352.
- [3] R.J. Pugh, *J. Colloid Interf. Sci.* 138 (1990) 16–20.
- [4] W.L. Vaughn, H.G. Maahs, *J. Am. Ceram. Soc.* 73 (6) (1990) 1540–1543.
- [5] P.E. Pehrsson, B.D. Thomas, *J. Vac. Sci. Technol. A* 15 (1997) 1–9.
- [6] V. Van Elsbergen, O. Janzen, W. Mönch, *Mater. Sci. Eng. B* 46 (1997) 366–369.
- [7] C. Öneby, C.G. Pantano, *J. Vac. Sci. Technol. A* 15 (1997) 1597–1602.
- [8] R. Moene, M. Makkee, J.A. Moulijn, *Appl. Catal. A* 167 (1998) 321–330.
- [9] A. Gözl, G. Horstmann, E. Stein von Kamienski, H. Kurz, *Proceeding of the Silicon Carbide and Related Materials 1995 Conference*, Inst. Phys. Conf. Ser. No. 142, Kyoto, Japan, 1995 (Chapter 3).
- [10] B.C. Mutsuddy, *J. Am. Ceram. Soc.* 73 (9) (1993) 2747–2749.
- [11] M. Rahaman, L.C. De Jonghe, *J. Am. Ceram. Soc. Bull.* 66 (5) (1987) 782–785.
- [12] G. Chauveteau, *J. Rheol.* 26 (2) (1982) 111–142.
- [13] G. Chauveteau, M. Tirrell, A. Omari, *J. Colloid Interf. Sci.* 100 (1) (1984) 41–54.
- [14] J.M. Powers, G.A. Somorjai, *Surf. Sci.* 244 (1991) 39–50.
- [15] R. Berjoan, J. Rodriguez, F. Sibieude, *Surf. Sci.* 271 (1992) 237–243.
- [16] B. Hornetz, H.-J. Michel, J. Halbritter, *J. Mater. Res.* 9 (1994) 3088–3094.
- [17] D. Schwarcz, R.A.M. Keski-Kuha, *Mater. Res. Soc. Symp. Proc.* 354 (1995) 535–540.
- [18] J. Lecourtier, L.T. Lee, G. Chauveteau, *Colloids Surf.* 47 (1990) 219–231.
- [19] A. Grosjean, M. Rezrazi, M. Tachez, *Surf. Coat. Technol.* 96 (1997) 300–304.
- [20] V. Médout-Marère, A. El Ghzaoui, C. Charnay, J.M. Douillard, G. Chauveteau, S. Partyka, *J. Colloid Interf. Sci.* 223 (2000) 205–214; V. Médout-Marère, S. Partyka, R. Dutartre, G. Chauveteau, J.M. Douillard, *J. Colloid Interf. Sci.* 262 (2003) 309–320.
- [21] L. Nabzar, J.P. Coste, G. Chauveteau, *Water quality and well injectivity*, in: *Proceedings of the Ninth European Symposium on Improved Oil Recovery*, The Hague, The Netherlands, October 20–22, 1997.
- [22] G. Chauveteau, L. Nabzar, J.P. Coste, *Physics and modeling of permeability damage induced by particle deposition*, in: *Proceedings of the SPE International Symposium on Formation Damage Control*, Lafayette, Louisiana, February 18–19, 1998.
- [23] P. Decourval, *Mémoire Ing. CNAM*, Paris, 1998.
- [24] N. Gnoevaya, L. Grozdanov, *Spis. Bulg. Geol. Druzh.* 26 (1965) 89.
- [25] V.M. Bermudez, *J. Appl. Phys.* 66 (1989) 6084–6092.
- [26] M. Sreemany, T.B. Ghosh, B.C. Pai, M. Chakraborty, *Mater. Res. Bull.* 33 (2) (1998) 189–198.
- [27] L. Filipuzzi, R. Naslain, C. Jaussaud, *J. Mater. Sci.* 27 (1992) 3330–3334.
- [28] D.R. Anderson, in: A.L. Smith (Ed.), *Analysis of Silicones*, John Wiley and Sons, New York, 1974, pp. 264–286.
- [29] J.S. Hartman, M.F. Richardson, B.L. Sheriff, B.G. Winsborrow, *J. Am. Chem. Soc.* 109 (1987) 6059–6067.
- [30] K.R. Carduner, R.O. Carter III, *Ceram. Int.* 15 (1989) 327.

- [31] C. Dybowski, E.J. Gaffney, A. Sayir, M.J. Rabinowitz, *Colloids Surf. A: Physicochem. Eng. Aspects* 118 (1996) 171–181.
- [32] S. Brunauer, P.H. Emmet, E. Teller, *J. Am. Chem. Soc.* 60 (1938) 309–319.
- [33] S.J. Gregg, K.S.W. Sing, *Adsorption, Surface Area and Porosity*, Academic Press, 1982.
- [34] P. Elder, V.D. Kestic, *J. Mater. Sci. Lett.* 8 (1989) 941.
- [35] T. Hase, B.W. Lin, T. Iseki, H. Suzuki, *J. Mater. Sci. Lett.* 5 (1986) 69.
- [36] A. Auroux, A. Gervasini, *J. Phys. Chem.* 94 (1990) 6371–6379.
- [37] S. Partyka, J.M. Douillard, *Pet. Sci. Eng.* 13 (1995) 95–102.
- [38] F.M. Fowkes, T.E. Burgess, in: G. Goldfinger (Ed.), *Clean Surfaces*, New York, 1970.
- [39] S. Partyka, F. Rouquerol, J. Rouquerol, *J. Colloid Interf. Sci.* 68 (1979) 21–31.
- [40] D.A. Griffiths, D.W. Fuerstenau, *J. Colloid Interf. Sci.* 80 (1981) 271–283.
- [41] T.W. Healy, D.W. Fuerstenau, *J. Colloid Interf. Sci.* 20 (1965) 376–386.